Passive Earth Pressure Transition Behind Retaining Walls

擁壁의 變位에 따른 靜止土壓에서 受動土壓까지의 變化

Kim, Hong-Taek*
金 洪 澤

要 旨

本 硏究에서는 靜止土壓狀態에서 受動土壓狀態 까지의 토압의 변화를 옹벽의 變位量에 따라 나타내는 새로운 이론이 제시되었다. 제시된 이론은 2次元平衡條件式과 Mohr-Coulomb의 破壞規準을 변형한 最大主應力과 最小主應力의 관계식을 바탕으로 이루어졌으며, 또한 옹벽의 變位量에 따른 흙의 내부마찰각(ϕ)과 벽마찰각(δ)의 변화를 옹벽上端에서 부터의 깊이의 함수로 나타내는 수학적 model이 개발되었다. 결과치를 수치해석적으로 구하기 위해 有限差分法이 이용되었고, 또한 얻어진 결과치를 실험치와 비교함으로써 本 硏究에서 제시된 이론의 適合性이 확인되었다. 옹벽 설계와 관련된 벽마찰각의 변화가 토압에서 미치는 영향에 대해서도 아울러 考察되었다.

ABSTRACT

An analytical solution procedure is described to estimate the developed passive lateral earth pressures behind a vertical rigid retaintng wall rotating about its toe into a mass of cohesionless soil. Various stages of wall rotation, starting from an at-rest state to an initial passive state to a full passive state, are considered in the analysis. Condition of failure defined by a modified Mohr-Coulomb criterion, together with equilibrium conditions, is used to obtain the necessary equations for the solution. Using methods of stress characteristics and numerical finite difference, a complete solution within and on the boundaries of the entire solution domain is made possible. The variations of the soil shear strength and the wall friction at various depths and stages of wall rotation are also taken into account in the analysis. The results predicted by the developed method of analysis are compared with those obtained from the experimental model tests on loose and dense sand. The comparisons show good agreements at various stages of retaining wall rotation. Finally, results of analytical parametric study are presented to demonstrate the effects of wall friction on the resultant thrust and distribution of developed lateral earth pressures.

INTRODUCTION

The estimation and prediction of the lateral earth pressure development has been one of the most

* 正會員, 弘益大學校 工科大學 土木工學科 助敎授

important aspects in geotechnical engineering. The development of active lateral earth pressures in particular has received a considerable amount of attention, since a majority of retaining structures are designed based on the active lateral earth pressures due to the tendency of outward movement. However, design of many geotechnical structures requires consideration of passive lateral earth pressures. Several analytical and experimental studies have been made in the past to investigate the magnitude and distribution of passive lateral earth pressures developed behind the retaining walls [3,5,7,8,12]. These studies have been very helpful for understanding the mechanism of the development of passive lateral earth pressures. However, most of the analytical studies fail to provide adequate comparisons with experimental model test results. This may be in part due to the uncertainties associated with the variations of the soil strength and the wall friction with respect to the magnitude of wall movement. A need for an analytical solution which takes into account the variation of materal properties at various stages of wall movement therefore has been realized.

This paper presents an analytical solution method which describes the transition of the passive lateral earth pressures from an "at-rest" state to an "initial passive" state to a "full passive" state behind a vertical rigid wall rotating about its toe into a mass of cohesionless soil. The at-rest state is defined as a stage of no wall movement. The initial passive state refers to a stage of wall rotation when only the soil element at the top of the wall experiences a sufficient amount of deformation (limiting deformation) to achieve a limiting passive condition. The full passive state occurs when the entire zone of soil elements from the top to the toe of the well are in limiting passive condition. The transition of the lateral earth pressures from an at-rest to a full passive state is discussed and the developed method of analysis is used to compare with the model test results. Furthermore, an analytical parametric study is made to investigate the effects of wall friction on the resultant thrust and distribution of lateral earth pressures at various stages of wall rotation.

THEORETICAL FORMULATION

The equilibrium in two-dimensional plane strain state[11] can be written in differential equations as

$$\frac{\partial \sigma_x}{\partial x}+\frac{\partial \tau_{xz}}{\partial z}=0$$
$$\frac{\partial \tau_{xz}}{\partial x}+\frac{\partial \sigma_z}{\partial z}=\gamma \qquad (1)$$

where the coordinate x is measured positive from the top of the retaining wall toward the backfill and the coordinate z is measured positive from the top of the retaining wall toward the toe. γ indicates the unit weight of the soil. It is obvious from Eq. 1 that an additional equation is necessary to solve for three unknown stresses. One can use any familiar failure criterion for this purpose, which will lead to the solution only at the limiting state, i.e., at failure. Sokolovskii[10] solved this problem with a Mohr-Coulomb failure criterion in 1965. In this paper however to describe the transition of the passive lateral earth pressures from an at-rest to a full passive state (limiting state), an assumption as the necessary third equation-a relationship between the major and minor principal

stresses-is made.

$$\frac{1-\sin\Psi}{1+\sin\Psi}=\text{principal stress ratio} \tag{2}$$

In Eq. 2 the angle Ψ describes the slope of the line tangent to the Mohr's stress circle (Fig. 1). Note that if the angle Ψ equals to $-\phi$ (internal soil friction angle), Eq. 2 reduces to Rankine's passive lateral earth pressure expression.

The angle Ψ is assumed to vary in magnitude from ϕ_0 to-ϕ, where ϕ_0 indicates the inclination angle relating σ_1 and σ_3 at at-rest state. Note that a negative magnitude of friction angle is used for the purpose of developing a general formulation, i.e., a positive friction angle describes the transition of active lateral earth pressures. If the at-rest lateral earth pressure coefficient, K_0, is known, the value of ϕ_0 can be easily obtained from

$$\sin\phi_0=\frac{1-K_0}{1+K_0} \tag{3}$$

Eq. 2 then becomes

$$\sigma_3=\sigma_1\frac{1-\sin\phi_0}{1+\sin\phi_0} \tag{4}$$

By varying the angle Ψ from ϕ_0 to-ϕ, Eq. 2 could represent both at-rest and full passive state. However, when the wall experiences movements other than translational, the resulting rotation may produce different principal stress ratios at various depths depending upon the stage of the wall rotation, e.g., portion(s) of the backfill soil whose deformations exceed the limiting value may achieve $\Psi=-\phi$ state, whereas the remaining portion may still have $\phi_0>\Psi>-\phi$ state. Therefore, the angle Ψ, describing the relationship between the major and minor principal stresses, may have to be described as a function of the depth, i.e., $\Psi=\Psi(z)$. Note that in reality Ψ may be a function of both x and z. However, the effect of x coordinate has been neglected for the purpose of obtaining an approximate solution. Based on this assumption and Mohr's coircle relationship, three unknown stresses can be expressed as

$$\begin{aligned}\sigma_x&=\sigma(1+\sin\Psi(z)\cos 2\theta)\\ \sigma_z&=\sigma(1-\sin\Psi(z)\cos 2\theta)\\ \tau_{xz}&=\sigma\sin\Psi(z)\sin 2\theta\end{aligned} \tag{5}$$

where $\sigma=\frac{\sigma_1+\sigma_3}{2}$ at any depth z

and θ=rotation angle from x-axis to the direction of σ_1 (Figs. 1 and 2).

Substitution of Eq. 5 into Eq. 1 yields

$$\frac{\partial\sigma}{\partial x}[1+\sin\Psi(z)\cos 2\theta]+\frac{\partial\sigma}{\partial z}\sin\Psi(z)\ \sin 2\theta$$
$$-2\sigma\sin\Psi(z)\left[\sin 2\theta\frac{\partial\theta}{\partial x}-\frac{1}{2}\ \frac{\sin 2\theta}{\tan\Psi(z)}\ \frac{\partial\Psi(z)}{\partial z}-\cos 2\theta\frac{\partial\theta}{\partial z}\right]=0 \tag{6}$$

$$\frac{\partial\sigma}{\partial x}[\sin\Psi(z)\sin 2\theta]+\frac{\partial\sigma}{\partial z}[1-\sin\Psi(z)\ \cos 2\theta]$$
$$+2\sigma\sin\Psi(z)\left[\cos 2\theta\frac{\partial\theta}{\partial x}-\frac{1}{2}\ \frac{\cos 2\theta}{\tan\Psi(z)}\ \frac{\partial\Psi(z)}{\partial z}+\sin 2\theta\frac{\partial\theta}{\partial z}\right]=\gamma \tag{7}$$

The point A in Fig. 1 indicates an orientation of the plane which satisfies $\sigma_n\tan\Psi(z)=\tau_n$. The rotation angle, μ, from the direction of σ_1 to this "pseudo-slip" plane therefore becomes

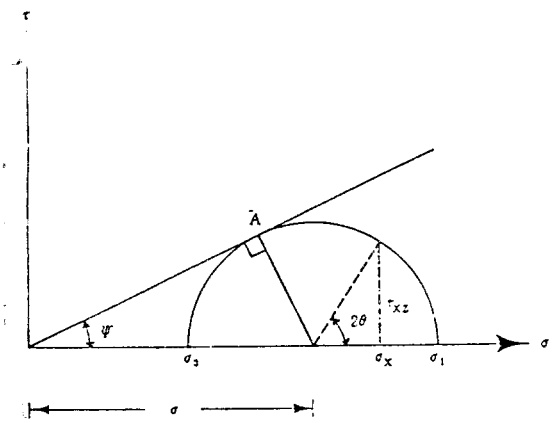

Fig. 1, Stress Relationship

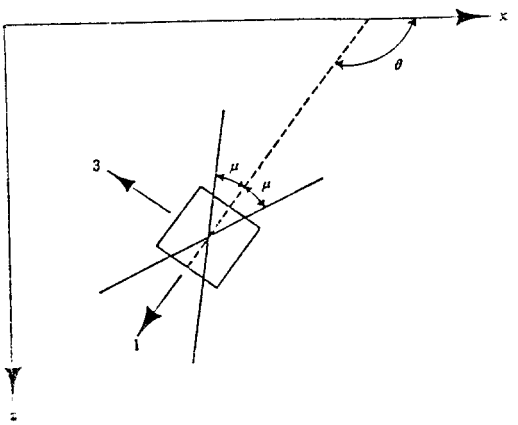

Fig. 2, Orientation of Pseudo-Slip Lines

$$\mu=\frac{\pi}{4}-\frac{\Psi(z)}{2} \tag{8}$$

as schematically shown in Fig. 2. Therefore the slope of the pseudo-slip line, $\frac{dz}{dx}$, becomes

$$\frac{dz}{dx}=\tan\ (\theta\pm\mu) \tag{9}$$

Multiplying Eq. 6 by $\frac{\sin(\theta\pm\mu)}{\cos\Psi(z)}$, Eq. 7 by $-\frac{\cos(\theta\pm\mu)}{\cos\Psi(z)}$ and adding, one can have

$$\left[\frac{\partial\sigma}{\partial x}\mp2\sigma\tan\Psi(z)\frac{\partial\theta}{\partial x}\pm\gamma\tan\Psi(z)\pm\sigma\frac{\partial\Psi(z)}{\partial z}\right]\cos(\theta\mp\mu)$$
$$+\left[\frac{\partial\sigma}{\partial z}\mp2\sigma\tan\Psi(z)\frac{\partial\theta}{\partial z}-\gamma\right]\sin\ (\theta\mp\mu)=0 \tag{10}$$

Multiplying Eq. 10 by $\frac{dx}{\cos(\theta\pm\mu)}$ and using Eq. 9, the following expressions are obtained.

$$d\sigma-2\sigma\tan\Psi(z)\,d\theta=\gamma[dz-\tan\Psi(z)\,dx]-\sigma\frac{\partial\Psi(z)}{\partial z}dx \tag{11}$$

$$d\sigma+2\sigma\tan\Psi(z)\,d\theta=\gamma[dz+\tan\Psi(z)\,dx]+\sigma\frac{\partial\Psi(z)}{\partial z}dx \tag{12}$$

According to Sokolovskii (10), the derivatives in Eqs. 9, 11, and 12 could be replaced by finite difference equivalents so as to find approximately the values of x, z, σ, and θ in three distinct regions as show in Fig. 3. These three distinct regions are formed by the pseudo-slip lines whose slopes are given in Eq. 9. Rewriting Eqs. 9, 11, and 12 in backward finite difference forms gives

$$z_{i,j}-z_{i-1,j}=(x_{i,j}-x_{i-1,j})\tan(\theta_{i-1,j}-\mu_{i-1,j}) \tag{13}$$

$$z_{i,j}-z_{i,j-1})=(x_{i,j}-x_{i,j-1})\tan(\theta_{i,j-1}+\mu_{i,j-1}) \tag{14}$$

$$(\sigma_{i,j}-\sigma_{i-1,j})-2\sigma_{i-1,j}(\theta_{i,j}-\theta_{i-1,j})\tan\Psi_{i-1,j}$$
$$=\gamma[(z_{i,j}-z_{i-1,j})-(x_{i,j}-x_{i-1,j})\ \tan\Psi_{i-1,j}]$$
$$-\sigma_{i-1,j}(x_{i,j}-x_{i-1,j})\frac{\partial\Psi}{\partial z}\Big|_{i-1,j} \tag{15}$$

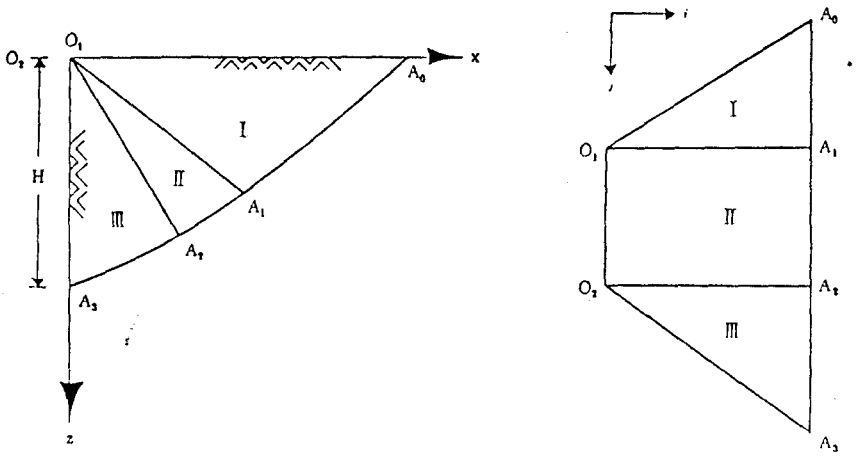

Pseudo-Slip Line Envelope　　Solution Domain

Fig. 3. Schematics of Solution Procedure

$$(\sigma_{i,j}-\sigma_{i,j-1})+2\sigma_{i,j-1}(\theta_{i,j}-\theta_{i,j-1})\tan\Psi_{i,j-1}$$
$$=\gamma[z_{i,j}-z_{i,j-1})+(x_{i,j}-x_{i,j-1})\tan\Psi_{i,j-1}]$$
$$+\sigma_{i,j-1}(x_{i,j}-x_{i,j-1})\frac{\partial\Psi}{\partial z}\Big|_{i,j-1} \qquad (16)$$

These four equations completely describe recurrence formulas for the determination of the pseudo-slip line coordinates ($x_{i,j}$ and $z_{i,j}$), the pseudo-slip line slope ($\theta_{i,j}\pm\mu_{i,j}$), and the associated average stress ($\sigma_{i,j}$) in terms of previous values at coordinates $(i-1,j)$ and $(i,j-1)$. With known values of x, z, σ, and θ at the boundaries, these recurrence formulas can be used to obtain solutions at all nodal points within the entire solution domain as shown in Fig. 3. Solution process starts from the line, O_1A_0, i.e., the ground surface whose coordinates and stress values are known, to the line O_2A_3, i. e., the rear face of the retaining wall, through regions Ⅰ, Ⅱ, Ⅲ. The detailed description of the solution procedure is beyond the scope of this paper; it is described in reference[10].

The detailed solution steps however require a description of the functionΨ (z) and its derivative, which define the transition of the lateral earth pressures from an at-rest to a full passive state. As discussed before the function varies from ϕ_0 at at-rest state to-ϕ at full passive state. The variation between these two extreme values is assumed as following.

Let β denote the stage of wall rotation so that $\beta=0$ for at-rest state $\beta=1.0$ for initial passive state, and $\beta=2.0$ for full passive state. In other words, for values of β between 0 and 1.0, transition from an at-rest to an initial passive state is described. Assuming that the behavior of the soil is elasto-fully plastic as defined by the limiting deformation, the values of β between 0 and 1.0 describe elastic behavior of the soil, since the limiting deformation of the soil does not develop yet. Therefore it can be assumed that the developed deformation of the soil for $0\leq\beta\leq1.0$ is directly proportional to β, i.e., elastic range.

Values of β between 1.0 and 2.0 describe the transition from an initial passive to a full passive state, i. e., elasto-plastic range. Fig. 4 shows the schematic variation of Ψ (z), where $(\beta-1)H$

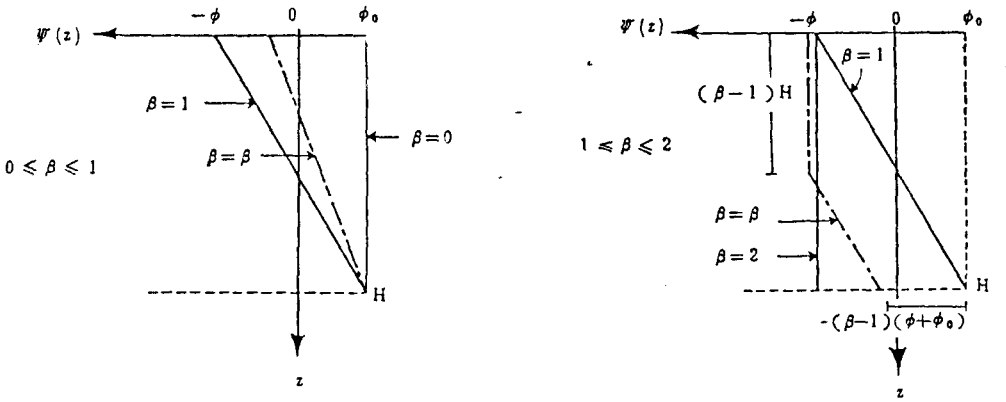

Fig. 4. Variation of $\Psi(z)$—Inward Toe Rotation

indicates the thickness of the soil from the ground surface which experiences deformations exceeding the limiting value. At $\beta=1.0$, the variation of $\Psi(z)$ is assumed to be $\Psi(z)=-\phi$ at $z=0$ and $\Psi(z)={}_0\phi$ at $z=H$, since by definition the initial passive state describes a stage of wall rotation when only the soil element at $z=0$ reaches a limiting passive condition. The original concept of this approach was first proposed by Dubrova as reported by Harr[4] in his "method of redistribution of pressures."

The variations of $\Psi(z)$ at various values of β assumed in the analysis can be expressed as for $0\leq\beta\leq1.0$, i. e., in elastic region,

$$\Psi(z)=\phi_0+(\phi-\phi_0)\frac{z}{H}\beta$$

$$\frac{\partial\Psi(z)}{\partial z}=\beta(\phi-\phi_0)\frac{1}{H} \tag{17}$$

For $1.0<\beta\leq2.0$

within zone already in limiting passive condition $[0\leq z\leq(\beta-1.0)H]$, i. e., in plastic region,

$$\Psi(z)=-\phi$$

$$\frac{\partial\Psi(z)}{\partial z}=0 \tag{18}$$

within zone not yet in limiting passive condition $[(\beta-1.0)\ H<z\leq H]$, i. e., in elastic region,

$$\Psi(z)=\phi_0-(\phi+\phi_0)\left(\beta-\frac{z}{H}\right)$$

$$\frac{\partial\Psi(z)}{\partial z}=(\phi+\phi_0)\frac{1}{H} \tag{19}$$

COMPARISON WITH MODEL TESTS

The developed method of analysis is used to compare with the model test results reported by Narain et al.[7]. The model wall was 1.5 ft. in height and made of structural steel. The tests were performed on dry "Ranipur sand", a typical river sand in India, with two different relative densities (Dr) of 31.5% and 70.25%. Hand tamping was used to obtain desirable soil densities. The model wall was rotated inward about the toe, and the developed passive lateral earth pressures

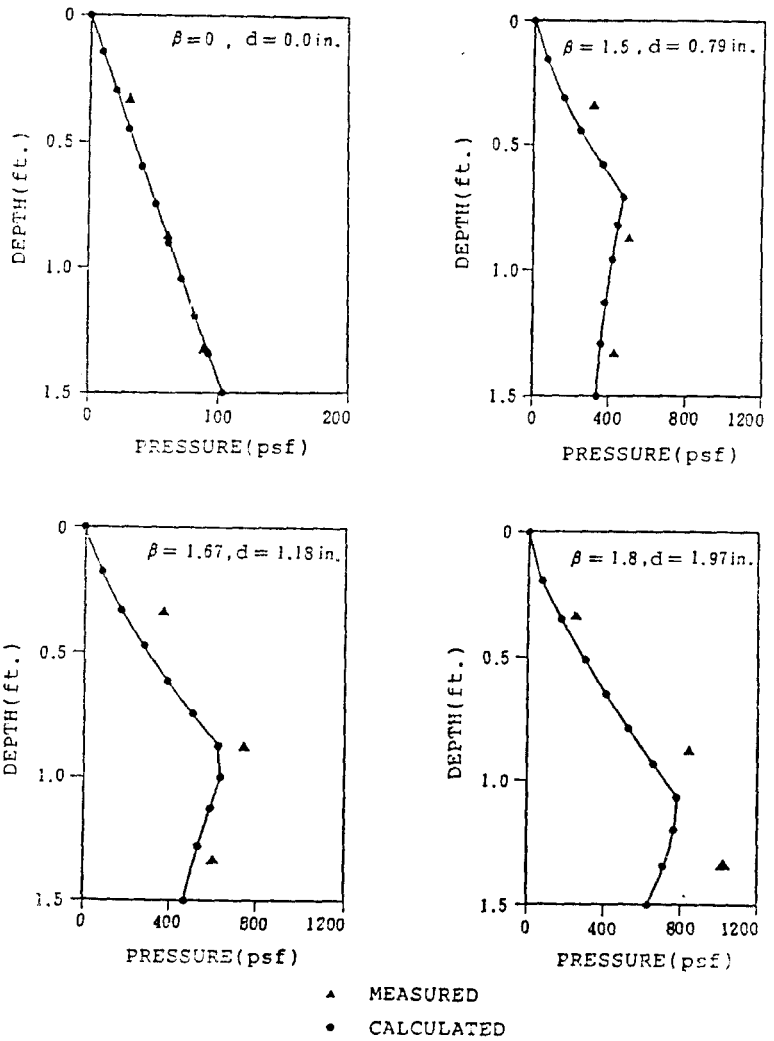

Fig. 5 Model Test Comparison for Loose Sand-Inward Toe Rotation

behind the wall at various displacements were measured using three soil pressure transducers, located at the depths of 0.33 ft., 0.88 ft., and 1.33 ft. from the top of the backfill. The displacements of the wall, d, as indicated in Figs. 5 and 6, were measured at its midheight.

Figs. 5 and 6 show the detailed comparisons of calculated and measured passive lateral earth pressures behind the wall at various stages of wall rotation. The internal friction angles of the sand and the wall friction angle reported by Narin et al.[7], together with other pertinent soil properties used in the analysis, are shown in Table 1. The values of initial at-rest lateral earth pressure coefficient, K_0, were obtained from the earth pressure distribution at-rest. The unit weights of the sand, however, were backcalculated from the relationship between the soil density and its angle of internal friction reported by Sherif et al.[9], since Narain et al. did not report these properties. The values of β, indicating the various stages of wall rotation as shown in the figures, were obtained from limiting deformations defining the passive state. The limiting defor-

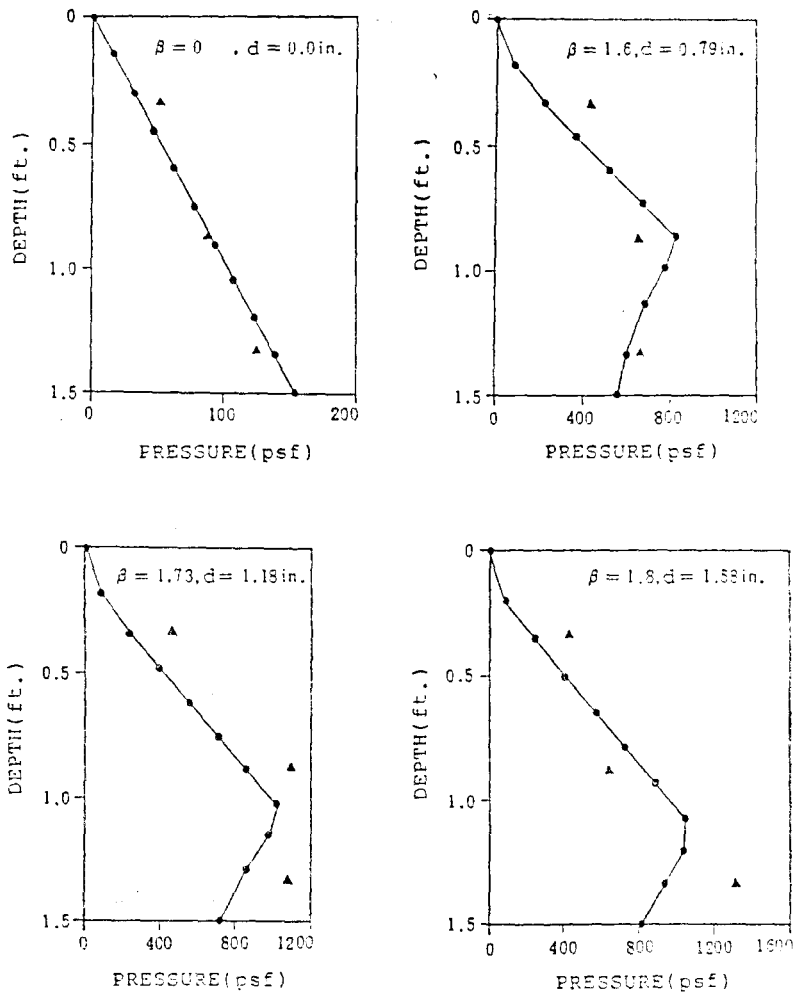

Fig. 6 Model Test Comparison for Dense Sand-Inward Toe Rotation

Table 1. Sand Properties-"Ranipur Sand"

Material Properties	Loose Sand	Dense Sand
ϕ	38.5°	42°
δ	23.5°	23.5°
K_0	0.69	0.96
γ	99.8pcf	106.1pcf

mations, as taken average values of measured deformations corresponding to at or near largest passive earth thrusts, reported by Narain et al., vary from 1.97 in. for loose sand to 1.58 in for dense sand at the midheight of the wall.

As illustrated in Figs. 5 and 6, the agreements are in general very good. However, near the toe of the wall with relatively large deformations the agreement is not as good-the measured lat-

eral earth pressure increases considerably with small increase in wall rotation unlike the measurements from other pressure cells. For instance, for wall rotations corresponding to β between 1.67 and 1.8 the lateral earth pressures measured at a depth of 1.33 ft. increase by about 71% (425 psf) for loose sand (Fig. 5) and by about 22% (237psf) for dense sand (Fig. 6), whereas the increases in calculated pressures for loose and dense sands are about 43% (214psf) and about 13% (109psf), respectively. It is also noted that parabolic-shaped pressure distributions are obtained during transition periods from both analytical and experimental results (Figs. 5 and 6) This supports many previous researchers' findings, both analytical and experimental, suggesting such a shaped pressure distribution.

PARAMETRIC STUDY

The developed method of analysis is further used to investigate the effect and significance of wall friction considered important in the design of retaining walls. To study analytically the effect of wall friction mobilization on the passive earth pressure coefficient (K_p), Graham[3] assumed several different wall friction angle distributions along the wall at passive state and constructed a chart showing calculated values of K_p as a function of soil friction angle (ϕ).

Table 2. Percentage Difference in Resultant Thrusts with Different Wall Friction Angles

Type of wall movement	Wall friction angle	$\beta=0.5$	$\beta=1.0$	$\beta=1.5$	$\beta=2.0$
Inward toe rotation	$\delta=0°$				
	$\delta=10°$	-1.74*	$+0.63$	$+9.68$	$+24.05$
	$\delta=20°$	-0.41	-0.23	$+11.5$	$+11.16$

β denotes the stage of wall rotation

* : $\frac{p_{\delta=10°}-p_{\delta=0°}}{p_{\delta=0°}}\times 100(\%)$

In the present study the effects of wall friction on the resultant thrust and distribution of developed lateral earth pressures at various stages of inward wall rotation about the toe are analyzed with three different wall roughnesses ($\delta=0°$, $\delta=\phi/3$, and $\delta=2/3\phi$). Table 2 summarizes the percentage difference in resultant thrusts between two different wall friction angles at various stages of wall rotation. These values are obtained with the following parameters:

Height of the wall (H) = 10ft.
At-rest earth pressure coefficient (K_0) = 0.5
Unit weight of the soil (γ) = 100pcf
Soil friction angle (ϕ) = 30°
Wall friction angle (δ) = 0°, 10°, 20°

Following observations can be made from this study:

1. From an at-rest ($\beta=0$) to an initial passive state ($\beta=1.0$) the resultant thrusts remain more or less the same for all degrees of wall roughness (Fig. 7). However, for wall rotations greater than $\beta=1.0$ the resultant thrusts increase with increasing wall friction.
2. In general the developed lateral earth pressures increase with increasing wall friction (Figs. 8 and 9).
3. The rate of increase in lateral earth pressures below the midheight of the wall generally incre-

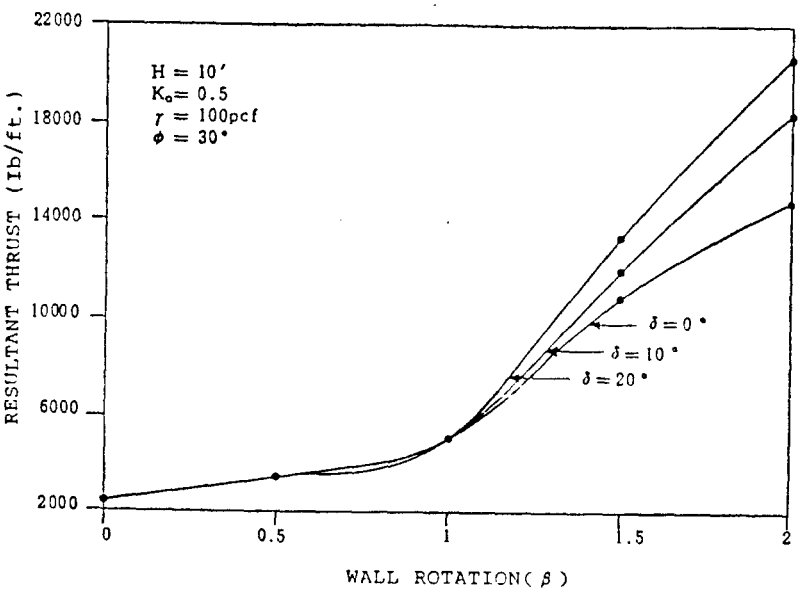

Fig.7 Variation of Resultant Thrust for Different Wall Friction-Inward Toe Rotation

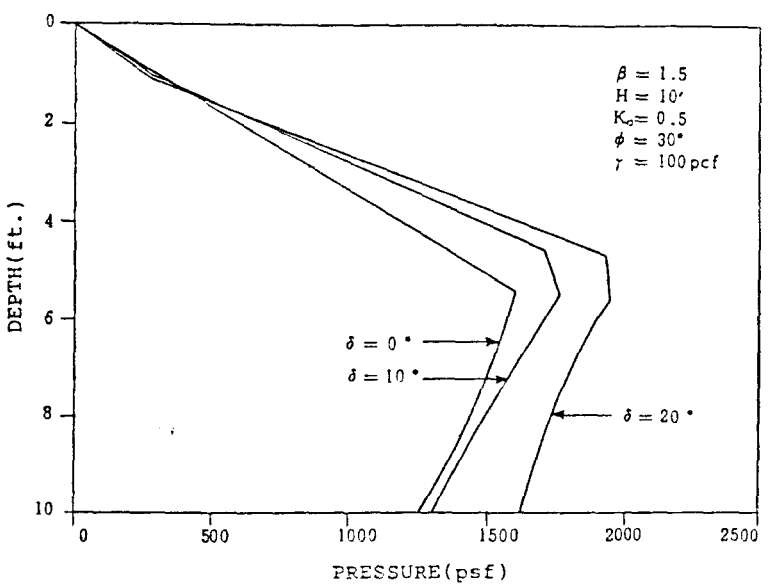

Fig.8 Variation of Lateral Earth Pressure for Different Wall Friction —-Inward Toe Rotation $\beta=(1.5)$

ases with increasing wall friction for wall rotation corresponding to $\beta=1.5$ (Fig. 8), whereas at $\beta=2.0$ (Fig. 9) this rate of increase decreases with increase in wall friction.

4. The developed lateral earth pressures near the upper portion of the wall remain nearly unaffected by the wall roughness (Figs. 8 and 9).

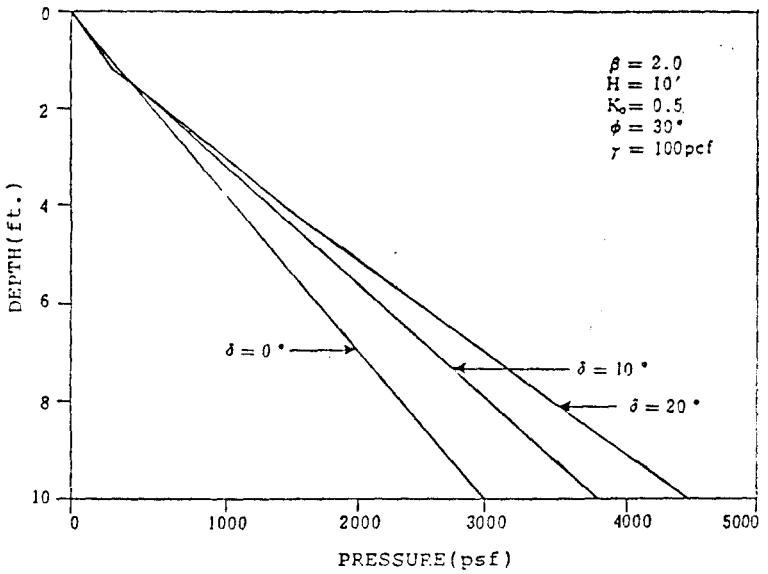

Fig. 9 Variation of Lateral Earth Pressure for Different Wall Friction —Inward Toe Rotation (β=2.0)

CONCLUSIONS

An analytical solution method which describes the transition of the lateral earth pressures from an at-rest to a full passive state behind a rigid retaining wall experiencing an inward rotation about the toe with horizontal cohesionless backfill soil, has been developed. The comparisons with model test results in general have shown good agreements, indicating the effectiveness of the developed formulation. Furthermore, an analytical parametric study has been made to investigate the effect and significance of wall friction on the resultant thrust and distribution of developed lateral earth pressures.

The developed solution method can be further expanded to analyze the transition of the lateral earth pressures associated with other types of wall movement, including the translation under active or passive condition. However, the developed analytical method of analysis includes many assumptions; namely, the limiting deformation to achieve a passive state, the validity of Mohr-Coulomb failure criterion, and the relationship between the major and minor principal stresses. These assumptions should therefore be studied further, as additional experimental data become available, so that the true behavior of the lateral earth pressure transition under various types of wall movement can be modeled more effectively. The effects of various parameters defining the system then can be analyzed in-depth through an additional parametric study.

ACKNOWLEDGEMENT

This work is a part of Author's Ph. D. dissertation. The Author overflows with gratitude for guidance, direction, and supervision bestowed by his advisor, Dr. S. Bang.

REFERENCES

1. Bang, S. and Kim, H.T., "Lateral Earth Pressure Development from At-Rest to Active Behind Retaining Walls," Proc., International Conference on Numerical Models in Geomechanics, Ghent, Belgium, April, 1986.
2. Bang, S. and Kim, H.T., "At-Rest to Active Earth Pressure Transition," A preprint presented at 65th Transportation Research Board Annual Meeting, Washington, D.C., January, 1986.
3. Graham, J., "Calculation of Passive Pressure in Sand," Canadian Geotechnical Journal, Vol. 8, 1971.
4. Harr, M.E., Foundations of Theoretical Soil Mechanics, McGraw-Hill Book Co., New York, NY., 1966.
5. James, R.G. and Bransby, P.L., "Experimental and Theoretical Investigations of a Passive Earth Pressure Problem," Geotechnique, Vol. 20, No. 1, 1970.
6. Kim, H.T., "Lateral Earth Pressure Development Behind Rigid Walls," Ph. D. Dissertation, South Dakota Tech., Rapid City, SD., 1987.
7. Narain, J., Saran, S., and Nandakumaran, P., "Model Study of Passive Pressure in Sand," Journal of the Soil Mechanics and Foundations Division, ASCE, Vol. 95, No. 4, July, 1969.
8. Rowe, P.W. and Peaker, K., "Passive Earth Pressure Measurements," Geotechnique, Vol. 15, No. 1, 1965.
9. Sherif, M.A., Ishibashi, I., and Lee, C.D., "Dynamic Earth Pressures Against Retaining Structures," Soil Engineering Research Report No. 21, Univ. of Washington, Seattle, January, 1981.
10. Sokolovskii, V.V., Statics of Granular Media, Pergamon Press, Oxford, 1965.
11. Timoshenko, S.P. and Goodier, J.N., Theory of Elasticity, McGraw-Hill Book Co., 3rd Ed., 1970.
12. Wong, K.S., "Elasto-Plastic Finite-Element Analyses of Passive Earth Pressure Tests," Ph. D. Dissertation, Univ. of California, Berkely, 1978.